

Cellular Uptake of *Clostridium botulinum* C2 Toxin: Membrane Translocation of a Fusion Toxin Requires Unfolding of Its Dihydrofolate Reductase Domain[†]

Gerd Haug, Christian Wilde, Jost Leemhuis, Dieter K. Meyer, Klaus Aktories, and Holger Barth*

Institut für Experimentelle und Klinische Pharmakologie und Toxikologie, Albert-Ludwigs-Universität Freiburg, Albertstrasse 25 (Otto-Krayer-Haus), D-79104 Freiburg, Germany

Received August 11, 2003; Revised Manuscript Received October 14, 2003

ABSTRACT: The *Clostridium botulinum* C2 toxin is the prototype of the family of binary actin–ADP-ribosylating toxins. C2 toxin is composed of two separated nonlinked proteins. The enzyme component C2I ADP-ribosylates actin in the cytosol of target cells. The binding/translocation component C2II mediates cell binding of the enzyme component and its translocation from acidic endosomes into the cytosol. After proteolytic activation, C2II forms heptameric pores in endosomal membranes, and most likely, C2I translocates through these pores into the cytosol. For this step, the cellular heat shock protein Hsp90 is essential. We analyzed the effect of methotrexate on the cellular uptake of a fusion toxin in which the enzyme dihydrofolate reductase (DHFR) was fused to the C-terminus of C2I. Here, we report that unfolding of C2I-DHFR is required for cellular uptake of the toxin via the C2IIa component. The C2I-DHFR fusion toxin catalyzed ADP-ribosylation of actin in vitro and was able to intoxicate cultured cells when applied together with C2IIa. Binding of the folate analogue methotrexate favors a stable three-dimensional structure of the dihydrofolate reductase domain. Pretreatment of C2I-DHFR with methotrexate prevented cleavage of C2I-DHFR by trypsin. In the presence of methotrexate, intoxication of cells with C2I-DHFR/C2II was inhibited. The presence of methotrexate diminished the translocation of the C2I-DHFR fusion toxin from endosomal compartments into the cytosol and the direct C2IIa-mediated translocation of C2I-DHFR across cell membranes. Methotrexate had no influence on the intoxication of cells with C2I/C2IIa and did not alter the C2IIa-mediated binding of C2I-DHFR to cells. The data indicate that methotrexate prevented unfolding of the C2I-DHFR fusion toxin, and thereby the translocation of methotrexate-bound C2I-DHFR from endosomes into the cytosol of target cells is inhibited.

Bacterial protein toxins, which modify their substrates in the cytosol of target cells, must develop strategies to transport their enzymatic domain across cellular membranes (1). Therefore, AB-type toxins show a bipartite organization with different functional domains, an enzyme domain (A) and a binding/translocation domain (B) (2). The B-domain mediates cell binding and the translocation of the A-domain into the cytosol. However, the mechanism by which the B-domain mediates translocation of the A-domain of bacterial toxins is still not completely understood.

In the family of binary ADP-ribosylating toxins, the A- and B-domains are two separated and nonlinked toxin components (for review see ref 3). Both components, the enzyme component and the binding component, have to assemble on the surface of the target cell to exhibit cytotoxic effects (4). The family of binary actin–ADP-ribosylating toxins consists of the *Clostridium botulinum* C2 toxin (5), *Clostridium perfringens* iota toxin (6, 7), *Clostridium spiroforme* toxin (7–9), *Clostridium difficile* ADP-ribosyltransferase (10, 11), and the VIP toxin (vegetative insecticidal protein) from *Bacillus cereus* (12). These toxins ADP-ribosylate G-actin at arginine-177 (13), leading to disas-

sembly of actin filaments, breakdown of the actin cytoskeleton, and rounding up of cultured monolayer cells (3, 14, 15).

In this study, we want to investigate the mechanism by which C2 toxin translocates into the cytosol of its target cells. C2 toxin is composed of the enzyme component C2I¹ (49 kDa) and the binding/translocation component C2II (80 kDa) (5), which has to be activated by trypsin cleavage (16). An ~20 kDa peptide is cleaved from the N-terminus, and the resulting active C2IIa (~60 kDa) forms ring-shaped heptamers in solution (17). The C2IIa heptamers bind to complex and hybrid carbohydrate structures on the surface of target cells (18). After assembly of C2I to C2IIa heptamers, the toxin complex is taken up via receptor-mediated endocytosis and reaches endosomal compartments. Upon acidification of endosomes, C2IIa forms pores in endosomal membranes, and C2I is delivered into the cytosol (17). However, it is still not known whether C2I translocates directly through the C2IIa pore [inner diameter 1–2 nm (17)]. If so, an (at least partial) unfolding of the C2I protein during translocation

[†] This work was supported by the Deutsche Forschungsgemeinschaft (SFB 388/C8 and SFB 505/B6).

* Corresponding author. Tel: +49-0761-2035308. Fax: +49-0761-2035311. E-mail: Holger.Barth@pharmakol.uni-freiburg.de.

¹ Abbreviations: Baf, bafilomycin A1; *C.*, *Clostridium*; C2I, enzyme component of *C. botulinum* C2 toxin; C2II, binding component of *C. botulinum* C2 toxin; DHFR, dihydrofolate reductase; HBSS, Hank's balanced salt solution; Hsp, heat shock protein; MTX, methotrexate; SDS–PAGE, sodium dodecyl sulfate–polyacrylamide gel electrophoresis.

should be expected. Moreover, we have recently shown that the cellular chaperone Hsp90 is required for translocation of C2I from endosomes into the cytosol (19), indicating that C2I is most likely transported in an unfolded conformation.

Here, we applied the dihydrofolate reductase (DHFR)/methotrexate (MTX) system, which is an established tool to study whether peptides have to be unfolded during a translocation process (20, 21). MTX is a folate analogue and favors a stable three-dimensional conformation of the DHFR (20). We report that cellular uptake of a fusion toxin, composed of C2I and DHFR, is diminished in the presence of MTX, suggesting that C2I-DHFR must become unfolded during C2IIa-mediated translocation into the cytosol of eukaryotic cells.

EXPERIMENTAL PROCEDURES

Materials. Oligonucleotides were obtained from MWG Biotech (Ebersberg, Germany). The pGEX-2T vector was included in the glutathione *S*-transferase gene fusion system from Pharmacia Biotech (Uppsala, Sweden). Polymerase chain reactions were performed with a T1 thermocycler from Biometra (Göttingen, Germany), and DNA sequencing was done with an ABI PRISM 310 genetic analyzer from Perkin-Elmer (Langen, Germany). Taq polymerase was purchased from Roche Molecular Diagnostics, glutathione-Sepharose 4B was from Pharmacia Biotech (Uppsala, Sweden), cell culture medium was from Biochrom (Berlin, Germany), fetal calf serum was from PAN Systems (Aidenbach, Germany), and MTX (dissolved in 0.1 N NaOH) and thrombin were from Sigma (Deisenhofen, Germany). Trypsin and trypsin inhibitor were from Roche Diagnostics (Mannheim, Germany). Phosphate-buffered saline (PBS) contained 8 g/L NaCl, 0.2 g/L KCl, 1.15 g/L Na₂HPO₄·2H₂O, and 0.2 g/L KH₂PO₄ (pH 7.4). Pierce Iodo-Beads were purchased from VWR International GmbH (Bruchsal, Germany), and Na¹²⁵I solution was from Hartmann Analytic (Braunschweig, Germany). Bafilomycin A1 was from Calbiochem (Bad Soden, Germany). Anti-rabbit F(ab')₂ fragment was purchased from Rockland.

Cloning of C2I-DHFR. For cloning of the C2I-DHFR construct, the original pGEX2TGI-C2I was used, which contains an internal *Bam*HI site (673 bp in C2I) and an in-frame stop codon, followed by a *Bam*HI site (22). First, the internal *Bam*HI site and the stop codon were mutated using the Quick-Change PCR kit (Stratagene, Germany) according to the manufacturer's instructions. Mouse DHFR gene (mDHFR; EMBL accession number L26316) was a gift from Dr. Nikolaus Pfanner (University of Freiburg, Germany). The gene was amplified with the primers mDHFR sense (5'-AGA TCT GCG GCC GCT ATG GTT CGA CCA TTG AAC TGC-3') and mDHFR anti (5'-AGA TCT GTC TTT CTT CTC GTA GAC TTC-3'), resulting in a 683 bp PCR product. By this method, we additionally introduced 9 bp at the 5' end of the mDHFR gene, which encode for three Ala residues that serve as a linker between mDHFR and C2I. The PCR product was subcloned into the pCR2.1 vector (Invitrogen, The Netherlands), mobilized by *Bgl*II digestion, and ligated into the digested pGEX2TGI-C2I vector, resulting in a 3' end fused DHFR gene. All mutations and cloning steps were confirmed by DNA sequencing (cycle sequencing ready reaction kit, Perkin-Elmer).

Expression, Purification, and Activation of Recombinant Proteins. C2I, C2II, and C2I-DHFR were expressed as GST fusion proteins in *Escherichia coli* BL21. Proteins were purified as described previously (22) and incubated with thrombin (3.25 NIH units/mL of bead suspension). Thereafter, the suspension was centrifuged, and an aliquot of the resulting supernatant was subjected to SDS-PAGE. Gels were stained with Coomassie Brilliant Blue R-250. C2II was purified as described elsewhere and activated with 0.2 µg of trypsin/µg of protein for 30 min at 37 °C (17).

Immunoblot Analysis. For detection of recombinant proteins, C2I (100 ng) and C2I-DHFR (200 ng) were subjected to SDS-PAGE and blotted onto nitrocellulose membrane (Schleicher & Schüll). The membrane was blocked with 3% non-fat-dried milk in PBST (PBS plus 0.05% Tween) overnight at 4 °C. Western blot analysis was performed with anti-C2I (polyclonal, rabbit, 1:5000 PBST) and anti-DHFR (polyclonal, rabbit, 1:1000 PBST) for 45 min at room temperature. Secondary goat anti-rabbit peroxidase coupled antibody was from Rockland, and visualization was performed using ECL reagent.

ADP-Ribosylation Assay. For determination of the enzymatic activity of C2I-DHFR, human platelet cytosol (about 50 µg of total protein) was incubated with thrombin-cleaved C2I-DHFR (0.2 nM final concentration) in a buffer containing 2 mM MgCl₂, 20 µM [³²P]NAD, and 50 mM HEPES (pH 7.3) for up to 8 min at 37 °C. For ADP-ribosylation in the presence of MTX, C2I-DHFR was preincubated with 20 µM MTX or 50 mM HEPES (pH 7.3) for 15 min at 4 °C. ADP-ribosylation of G-actin was performed as described above. Radiolabeled proteins were resolved by SDS-PAGE and further analyzed by using a phosphorimager.

Trypsin Digest of C2I-DHFR, C2I, and C2II with or without MTX. One microgram of protein was preincubated for 15 min at 37 °C with or without MTX (20 µM) or NaOH. Five microliters of trypsin solution (20 ng/mL) or PBS was added, and samples were incubated at 37 °C for 20 min. Samples were subjected to 12.5% SDS-PAGE with subsequent Coomassie staining. Western blot analysis was performed with an antiserum raised against C2I protein (polyclonal, rabbit, 1:5000 in PBST) or with an antibody against DHFR (polyclonal, rabbit, affinity purified, 1:500 in PBST; a gift of Dr. Wolfgang Voos, University of Freiburg) for 1 h at room temperature. Secondary goat anti-rabbit peroxidase coupled antibody was from Rockland, and visualization was performed using the enhanced chemiluminescence light system.

Cell Culture and Cytotoxicity Assay. Vero cells were cultivated in tissue culture flasks at 37 °C and 5% CO₂ in Dulbecco's MEM (DMEM) supplemented with 10% fetal calf serum, 100 units/mL penicillin, and 100 µg/mL streptomycin. Cells were routinely trypsinized and reseeded three times a week. For cytotoxicity assays, cells were grown as subconfluent monolayers. For comparison of C2I-DHFR and C2I, cells were incubated in serum-free DMEM together with C2IIa (concentrations as indicated) at 37 °C. To investigate the effect of MTX on intoxication of Vero cells with either C2I-DHFR (+C2IIa) or C2I (+C2IIa), the enzyme components were preincubated with MTX (concentration as indicated) for 15 min at 4 or 37 °C in 100 µL of serum-free DMEM and then added to serum-free DMEM containing MTX (same concentration) and C2IIa. The final concentra-

tions of toxin components and MTX present in the medium are given. Cells were further incubated at 37 °C, and the percentage of cell rounding was determined from microscopic pictures. For direct translocation of C2I-DHFR across the plasma membrane via C2IIa, precooled Vero cell monolayers (which were pretreated with 100 nM bafilomycin for 1 h at 37 °C) were incubated in serum-free DMEM containing C2I-DHFR (200 ng/mL) + C2IIa (400 ng/mL) with or without 20 μ M MTX for 1 h at 4 °C to allow toxin binding. Medium was removed, acidic medium (pH 5.2) at 37 °C was added, and cells were kept at 37 °C for 5 min. The acidic medium was removed, and cells were further incubated in serum-free DMEM with (or without, control) Baf and with or without MTX at 37 °C for intoxication for the indicated times. Astrocyte cultures were obtained from newborn Wistar rats (23). After isolation of the cortices of the rat brains, the surrounding meninges were removed prior to mincing. The fragments were incubated with 0.25% trypsin in phosphate-buffered saline (PBS; 8.1 mM Na₂HPO₄, 1.5 mM KH₂PO₄, 137 mM NaCl, and 2.7 mM KCl, pH 7.5) at 37 °C for 10 min. The enzymatically treated fragments were then dissociated into single cells by pipetting, and the cells were suspended in DMEM containing 10% fetal bovine serum, 5 mM HEPES buffer, and 0.2 mg/L LPS. The cells were maintained at 37 °C in 8.6% CO₂ for 10 days.

Immunocytochemistry. Cells were fixed with methanol (−20 °C) for 10 min, washed with PBS, and permeabilized with 0.1% (v/v) Triton X-100. Normal goat serum was used to block unspecific reactions. Thereafter, cells were incubated with the primary polyclonal rabbit anti-C2 toxin antibody. The C2 toxin immune complexes were visualized by using a CyTm 3-conjugated F(ab')₂ fragment of goat anti-rabbit IgG (Dianova, Hamburg, Germany). Cells were visualized by using a Bio-Rad (Hercules, CA) MRC 1024 (version 3.2) confocal system with a krypton–argon laser and a Zeiss (Oberkochen, Germany) Axiovert 135TV microscope. Images were obtained by using laser sharp 2.1T software and processed by using the Metamorph 6.1 Software (Visitron, Munich, Germany). The intensity of the C2 toxin staining in the endosomes was compared with the intensity in the cytosol by using the Metamorph 6.1 software. Single z-stack micrographs were obtained with identical settings from the confocal system. The intensity of staining of five endosomes per cell was measured and compared with the intensity of five randomly chosen areas per cell in the cytosol. Ten cells were analyzed for each treatment group in this way. The average of the intensity of the endosome staining was set as 100% for each group and was compared with the cytosol group. For actin staining, cells were fixed with 4% paraformaldehyde for 20 min, washed with PBS, and permeabilized with 0.1% (v/v) Triton X-100 for 30 min. Afterward, the cells were incubated with TRITC-conjugated phalloidin (Biozol, München, Germany) and washed again with PBS. Cells were visualized by using a Axiovert/Axiophot System (Zeiss, Oberkochen, Germany) processed by using the Metamorph 6.1 software (Visitron, Munich, Germany).

Labeling of C2I-DHFR with ¹²⁵I. Iodination of C2I-DHFR was performed with Iodo-Beads according to the manufacturer's (Pierce) protocol using 100 μ Ci of Na¹²⁵I/100 μ g of protein. In vivo activity of ¹²⁵I-C2I-DHFR was checked by incubation of cells together with C2IIa.

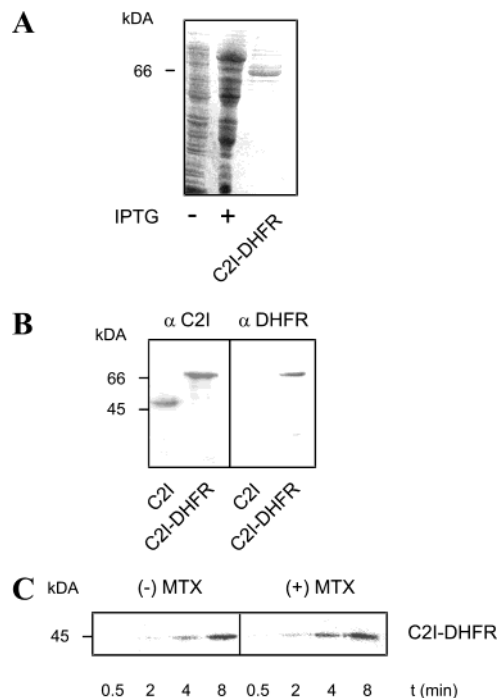


FIGURE 1: Expression, purification, and enzymatic activity of C2I-DHFR. (A) C2I-DHFR was expressed and purified as described under Experimental Procedures. An aliquot of the culture was taken before and 20 h after the addition of IPTG and subjected to SDS–PAGE, and that gel was stained with Coomassie blue. After induction with IPTG, GST-C2I-DHFR was obtained at the upper part of the gel (MG 98 kDa). Purification and cleavage with thrombin resulted in C2I-DHFR with an expected molecular mass of 71 kDa. (B) C2I (100 ng) and C2I-DHFR (200 ng) were analyzed by Western blot analysis. The respective proteins were separated by SDS–PAGE, blotted onto nitrocellulose, and probed with either rabbit anti-C2I (1:5000 PBST) or rabbit anti-DHFR (1:1000 PBST). Visualization was performed using ECL reagent. (C) Enzymatic activity of C2I-DHFR. Human platelet cytosol was preincubated with methotrexate (20 μ M final concentration) or 50 mM HEPES (pH 7.3) followed by [³²P]ADP-ribosylation with C2I-DHFR (0.2 nM final concentration) for up to 8 min at 37 °C. Probes were subjected to SDS–PAGE, and the autoradiograph is shown.

Binding of ¹²⁵I-C2I-DHFR to Vero Cells. ¹²⁵I-C2I-DHFR was preincubated in serum-free DMEM without or with various concentrations of MTX for 15 min at 4 °C. It was added to the Vero cell monolayers (12-well dish) containing C2IIa with or without MTX in serum-free DMEM. Final concentrations in the medium were 200 ng/mL ¹²⁵I-C2I-DHFR and 400 ng/mL C2IIa without or with various concentrations of MTX (concentration as indicated). Cells were incubated for 2 h at 4 °C, washed two times with 1 mL of PBS per well, and collected in 25 μ L of SDS sample buffer (95 °C). Equal amounts of lysate protein (~50 μ g) were subjected to 12.5% SDS–PAGE, and ¹²⁵I-C2I-DHFR was detected with a phosphorimager from Molecular Dynamics/Pharmacia (Freiburg, Germany).

RESULTS

Cloning and Characterization of the C2I-DHFR Fusion Toxin. The recombinant GST-C2I-DHFR fusion toxin was purified as described under Experimental Procedures, and the GST tag was removed by thrombin cleavage. The resulting C2I-DHFR protein was subjected to SDS–PAGE, resulting in a protein with the expected molecular mass of 71 kDa (Figure 1A). Furthermore, C2I-DHFR was tested by

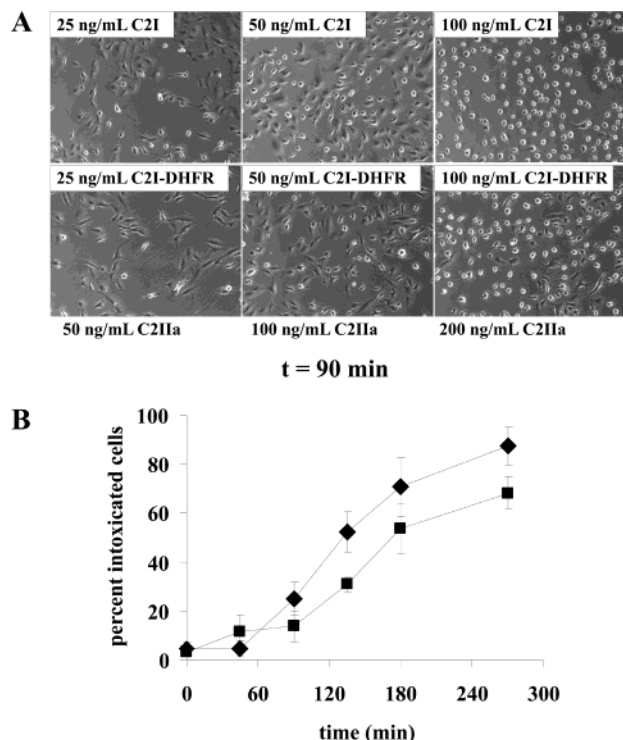


FIGURE 2: In vivo activity of C2I-DHFR. (A) Vero cells were incubated with increasing concentrations of C2I or C2I-DHFR and C2IIa. Cells were incubated at 37 °C, and photographs were taken after 90 min. (B) Vero cells were incubated with C2I (25 ng/mL) and C2IIa (50 ng/mL) or C2I-DHFR (25 ng/mL) and C2IIa (50 ng/mL). Photographs were taken at the indicated times (◆, C2I + C2IIa; ■, C2I-DHFR + C2IIa), and the percentage of intoxicated cells is given as the mean value \pm SD ($n = 3$).

immunoblot analysis and was recognized by a specific antiserum either against C2I or against DHFR, respectively (Figure 1B). Next, the *in vitro* ADP-ribosyltransferase activity of C2I-DHFR was tested. Therefore, human platelet cytosol (actin concentration $\sim 1 \mu\text{M}$) was incubated with C2I-DHFR (0.2 nM) in the presence of [*adenylate*- ^{32}P]NAD. As shown in Figure 1C, G-actin was ADP-ribosylated by the fusion toxin in a time-dependent manner. Because the catalytic domain of C2I is located in the C-terminal part of the protein, it was important to exclude that binding of MTX to DHFR did not interfere with ADP-ribosyltransferase activity of C2I-DHFR. To exclude this, we preincubated C2I-DHFR with MTX (20 μM final concentration) and performed the ADP-ribosylation reaction as described above. We obtained the same results as with the untreated protein, indicating that binding of MTX to C2I-DHFR did not alter the enzymatic activity of the fusion toxin (Figure 1C).

Cytotoxic Effects of C2I-DHFR Fusion Toxin. To test whether C2I-DHFR was translocated into the cytosol of target cells by activated C2II (C2IIa), we used intoxication of cells as a functional assay. Therefore, cultured Vero cells were incubated at 37 °C with the indicated amounts of C2I-DHFR together with C2IIa, and cells were photographed after 90 min. The first alterations in cell morphology were observed when 25 ng/mL C2I-DHFR plus 50 ng/mL C2IIa was used, and with 50 ng/mL C2I-DHFR plus 100 ng/mL C2IIa, cells started to round up. In a concentration of 100 ng/mL C2I-DHFR plus 200 ng/mL C2IIa, the intoxication of cells was nearly complete after 90 min (Figure 2A, lower panel). As a control, cells were treated with C2I plus C2IIa

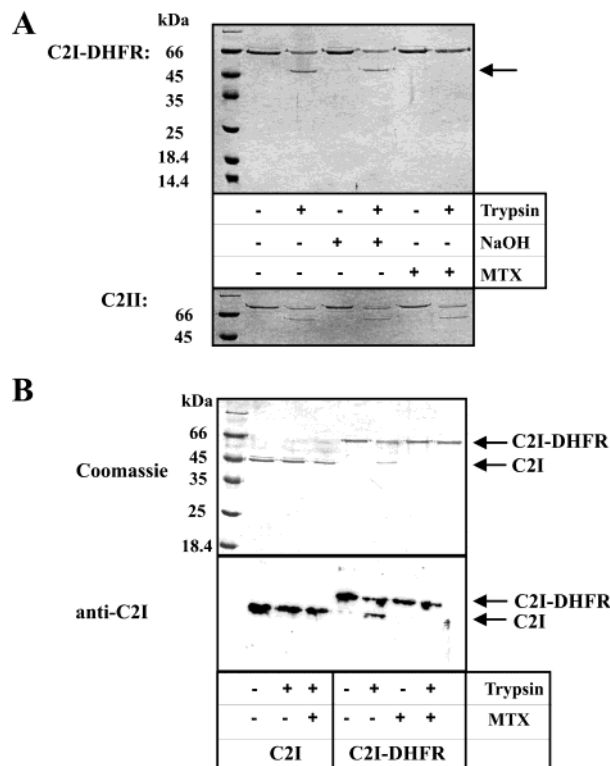


FIGURE 3: Trypsin digest of C2I-DHFR. (A) C2I-DHFR (1 μ g, upper panel) or C2II (1 μ g, lower panel) was preincubated without or with MTX or NaOH for 15 min at 37 $^{\circ}$ C. Trypsin (100 ng) or PBS was added, and samples were incubated for 20 min at 37 $^{\circ}$ C. Samples were analyzed by 12.5% SDS-PAGE. Coomassie-stained gels are shown. (B) C2I-DHFR (1 μ g) or C2I (1 μ g) was preincubated with or without MTX or NaOH for 15 min at 37 $^{\circ}$ C. Trypsin (100 ng) or PBS was added, and samples were incubated for 20 min at 37 $^{\circ}$ C. Samples were analyzed by 12.5% SDS-PAGE (upper panel) and by immunoblot analysis with an antiserum against C2I (lower panel).

under identical conditions, showing that C2I wild type acts in a comparable concentration range (Figure 2A, upper panel). Moreover, the single components C2IIa, C2I-DHFR, and C2I alone had no effects on cell morphology (data not shown). Figure 2B shows a time course of the percentage of intoxicated cells following treatment with either C2I (25 ng/mL) plus C2IIa (50 ng/mL) or C2I-DHFR (25 ng/mL) plus C2IIa (50 ng/mL). As shown, the cytotoxic activities of both toxins were comparable, indicating that C2I-DHFR is translocated into the cytosol of target cells with an efficiency similar to that of the C2I wild-type protein.

Effect of MTX on the C2I-DHFR Fusion Toxin. To test whether binding of MTX to C2I-DHFR favors a stable three-dimensional conformation of the DHFR domain, a protective effect of MTX on the tryptic digest of C2I-DHFR was tested. When C2I-DHFR was treated for 15 min at 37 °C with trypsin (100 ng/ μ g of protein) and subsequently subjected to SDS-PAGE, a second lower migrating protein band (indicated with an arrow) was obtained in the Coomassie-stained gel, which was due to cleavage of C2I-DHFR (Figure 3A, upper panel). In contrast, no degradation of C2I-DHFR was detected after pretreatment with MTX (20 μ M) prior to addition of trypsin. It is noteworthy that the protective effect of MTX is specific since (i) NaOH (in which MTX is diluted) had no effect on trypsin action and (ii) MTX did not protect C2II protein from tryptic digest (Figure 3A, lower panel). These results clearly indicate that MTX specifically stabilizes

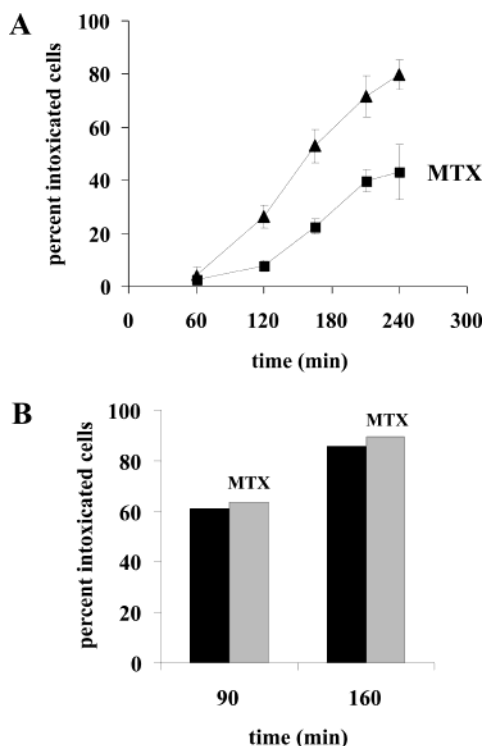


FIGURE 4: (A) Effect of MTX on C2I-DHFR/C2IIa cytotoxicity. Vero cells were incubated in serum-free DMEM containing 50 ng/mL C2I-DHFR and 100 ng/mL C2IIa with or without MTX at 37 °C. Pictures were taken after the indicated times, and the percentage of intoxicated cells was determined from the photographs (▲, toxin; ■, toxin + MTX). Given are the mean values \pm SD ($n = 3$). (B) Effect of MTX on C2I/C2IIa cytotoxicity. Vero cells were incubated with 50 ng/mL C2I and 100 ng/mL C2IIa with or without MTX at 37 °C for the indicated times. The percentage of intoxicated cells was determined from the photographs. The result of a representative experiment is shown.

the C2I-DHFR structure. Moreover, only the DHFR domain of the fusion toxin was digested by trypsin because C2I was resistant to trypsin digest under these conditions (Figure 3B). SDS-PAGE and subsequent Coomassie staining of trypsin-digested C2I-DHFR showed a resulting protein band, which was migrating in SDS-PAGE like C2I (Figure 3B, upper panel). This protein was recognized by an anti-C2I antiserum (Figure 3B, lower panel). An antibody against DHFR recognized neither C2I nor the resulting protein following trypsin digestion of C2I-DHFR (not shown).

Effect of MTX on C2I-DHFR Cytotoxicity. To determine whether MTX prevents cytotoxicity of C2I-DHFR and whether the stabilized three-dimensional DHFR domain affects C2IIa-mediated translocation of C2I-DHFR, Vero cells were incubated with C2IIa together with the MTX-pretreated C2I-DHFR fusion toxin (15 min at 4 °C) in the presence of MTX. For control, cells were incubated with C2I-DHFR plus C2IIa without MTX. After the indicated times, pictures were taken, and the percentage of intoxicated cells was determined from the pictures. In Figure 4A, a representative experiment is shown. In the presence of MTX, a significant delay of intoxication was observed. After 4 h or more, about 40% of the cells were intoxicated when MTX was present compared to about 80% of intoxicated cells without MTX. However, the MTX-induced delay in intoxication of cells was transient. When MTX was present, after 6 h of incubation, about 40% of the cells were intoxicated

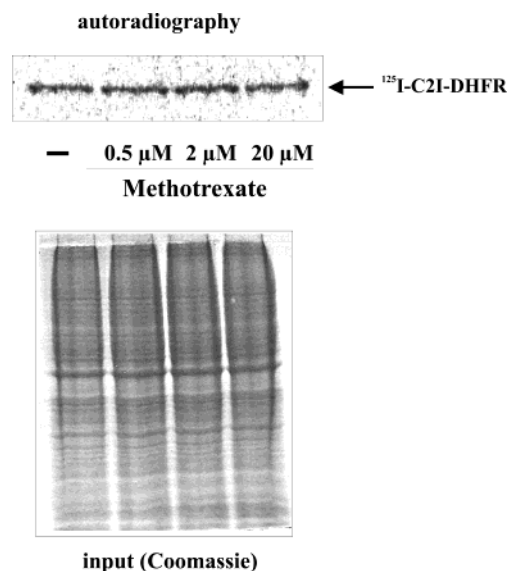


FIGURE 5: Binding of 125 I-C2I-DHFR on Vero cells. Cells were incubated in serum-free DMEM containing 200 ng/mL 125 I-C2I-DHFR and 400 ng/mL C2IIa with or without increasing concentrations of MTX for 2 h at 4 °C. Cells were washed and collected in SDS sample buffer, and equal amounts of the cell lysate were subjected to SDS-PAGE. Cell-bound 125 I-C2I-DHFR was detected in an autoradiograph, which is shown.

(without MTX, about 100% of cells were intoxicated; not shown), and after 24 h, all cells (with or without MTX) were intoxicated (not shown). The inhibitory effect of MTX on cytotoxicity of C2I-DHFR was due to its binding to the DHFR domain of the fusion toxin because MTX addition did not influence cytotoxicity of wild-type C2I/C2IIa (Figure 4B). Similar results were obtained with CHO cells (data not shown). To exclude that MTX decreased the binding of C2I-DHFR to cell-bound C2IIa, Vero cells were incubated with C2IIa and radiolabeled 125 I-C2I-DHFR for 2 h at 4 °C in the presence of increasing concentrations of MTX. Cells were lysed, and equal amounts of the lysate protein were subjected to SDS-PAGE (Figure 5, lower panel), and subsequently, the cell-bound radioactivity was detected by autoradiography (Figure 5, upper panel). Even 20 μ M MTX did not diminish C2IIa-mediated binding of C2I-DHFR to Vero cells. Binding of C2I-DHFR to cells was specific because no binding of C2I-DHFR was detected in the absence of C2IIa (not shown).

Effect of MTX on the Direct C2IIa-Mediated Translocation of C2I-DHFR across Cell Membranes. The specific inhibitor Baf blocks the vesicular H^+ -ATPase in endosomal membranes and thereby prevents acidification of endosomes. Therefore, Baf prevents intoxication of cells by C2 toxin (17). Direct translocation of C2I via C2IIa across the plasma membrane was achieved, even in the presence of Baf, when cell-bound C2 toxin was subjected to acidic medium (pH <5.6) (17). This way, the endosomal situation is mimicked at the cell surface (Figure 6A). Here, we used this assay to investigate whether the translocation step of C2I-DHFR across the endosomal membrane upon acidification is blocked by MTX. C2I, C2I-DHFR (pretreated for 15 min at 4 °C with 20 μ M MTX), and C2IIa are allowed to bind to cells, which have been pretreated with Baf (1 h, 37 °C) at 4 °C for 1 h in the presence or absence of MTX. The cells were shifted to 37 °C at pH 5.2 for 5 min to allow insertion of C2IIa pores into the plasma membrane and translocation of

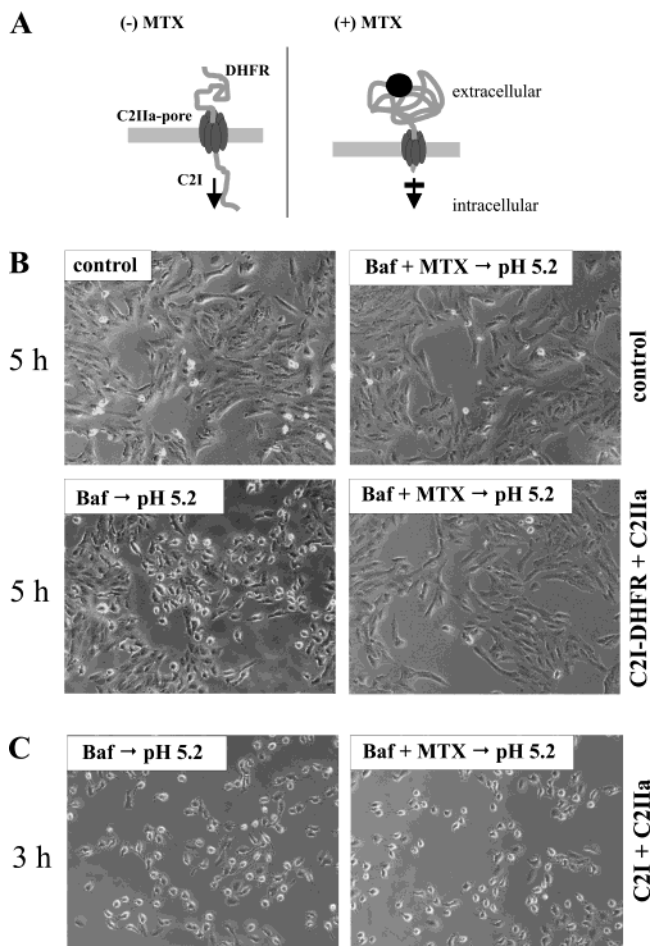


FIGURE 6: Direct translocation of C2I-DHFR across the plasma membrane via C2IIa. (A) Model of the translocation and unfolding of C2I-DHFR directly across the cell membrane. Under acidic conditions, C2IIa inserts into cell membranes and forms pores, and C2I is delivered into the cytosol of target cells. This assay mimics the endosomal situation on the cell surface. Pore formation by C2IIa, which is induced by acidification, and unfolding of C2I-DHFR are essential prerequisites for translocation of the toxin into the cytosol. However, it is not clear whether C2I translocates through the C2IIa pores. Cytotoxic effects of C2I-DHFR/C2IIa (B) and of C2I/C2IIa (C) on Vero cells after direct translocation of C2I-DHFR across the plasma membrane. Following binding of C2I-DHFR (B) or C2I (C) and C2IIa on precooled cells (pretreated with 100 nM Baf) for 1 h at 4 °C with or without MTX, cells were shifted for 5 min at 37 °C at pH 5.2. Medium was removed, and for intoxication, cells were incubated at 37 °C in DMEM with or without Baf and with or without MTX ($t = 0$). After the indicated time, pictures were taken.

C2I-DHFR across the plasma membrane into the cytosol. Medium was removed, and cells were incubated at 37 °C in serum-free DMEM containing Baf with or without MTX. In the presence of MTX, intoxication of cells was blocked after 5 h (Figure 6B). Control cells were not influenced by a treatment with Baf, MTX, and low pH (Figure 6B). To demonstrate that the inhibitory effect of MTX on the C2IIa-mediated translocation of the C2I-DHFR fusion toxin across cell membranes was dependent on its DHFR domain and therefore specific for C2I-DHFR, the influence of MTX on the C2IIa-mediated translocation of C2I was tested. When this experiment was performed with C2I instead of C2I-DHFR, no delay in intoxication of cells was observed in the presence of MTX (Figure 6C).

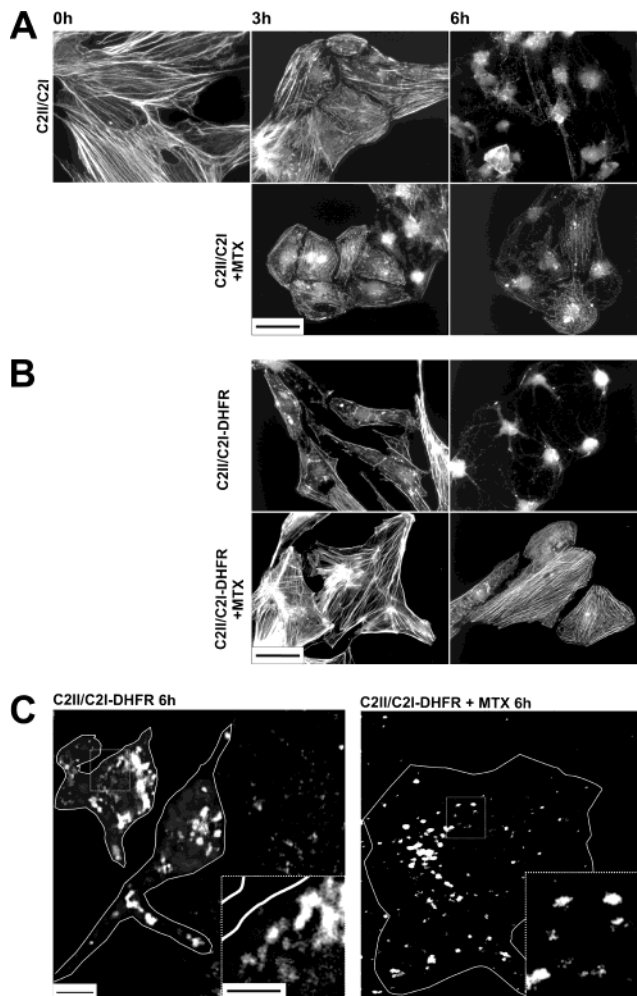


FIGURE 7: Influence of MTX on effects of C2I-DHFR/C2IIa toxin on rat astrocytes. (A) Effect of MTX on intoxication of astrocytes by C2I/C2IIa. Rat astrocytes were incubated for 3 or 6 h at 37 °C with C2I/C2IIa (200 ng/mL C2I + 400 ng/mL C2IIa) and in the presence of MTX (20 μ M). Cells were fixed with 4% PFA, and immunohistochemistry with TRITC-phalloidin was performed to stain F-actin (scale bar: 25 μ m). (B) Effect of MTX on intoxication of astrocytes by C2I-DHFR/C2IIa. Rat astrocytes were incubated for 3 or 6 h at 37 °C with C2I-DHFR/C2IIa (200 ng/mL C2I-DHFR + 400 ng/mL C2IIa) and in the presence of MTX (20 μ M). Cells were fixed with 4% PFA, and immunohistochemistry with TRITC-phalloidin was performed to stain F-actin (scale bar: 25 μ m). (C) Rat astrocytes were incubated for 6 h at 37 °C with C2I-DHFR/C2IIa toxin (200 ng/mL C2I-DHFR + 400 ng/mL C2IIa) in the presence of MTX (20 μ M). Cells were fixed with methanol, and immunohistochemistry with an anti-C2I antibody was performed. Thin-layer single z-stack confocal micrographs were taken from single cells (scale bar: 5 μ m).

Effect of MTX on Intracellular Localization of C2I-DHFR. Because MTX prevented translocation of C2I-DHFR into the cytosol directly across cell membranes, we tested whether C2I-DHFR was trapped in endosomes when MTX was present during the incubation of cells with C2I-DHFR plus C2IIa. The intracellular localization of C2I-DHFR was detected by confocal microscopy. For these experiments, we used rat astrocytes because these cells are larger and show a clearer distribution of cell compartments than Vero cells. When rat astrocytes were treated with C2 toxin (50 ng/mL C2I + 100 ng/mL C2IIa) for 6 h, cells rounded up and the actin cytoskeleton is redistributed (Figure 7A) (19). The effect of C2I/C2IIa was not influenced by MTX (Figure 7A).

When astrocytes were treated with C2IIa plus C2I-DHFR in the presence of MTX, cell rounding was influenced, and the actin filaments were still detectable after 6 h of incubation (Figure 7B). MTX did not block cytotoxic action of C2I-DHFR/C2IIa completely but delayed intoxication of the rat astrocytes. When cells were treated for 6 h with C2I-DHFR/C2IIa in the presence of MTX, there was less fusion of the endosomal-like compartments and less C2I-DHFR was detectable in the cytosol (Figure 7C). No cross-reactivity of the anti-C2I antibody with the C2IIa component was detectable (data not shown). Colocalization studies of C2I with the early endosomal marker Rab5 proved that these punctual structures were indeed endosomes (19). Next, we used the Metamorph software to measure the intensity of the C2 toxin staining in the endosomal compartments and compared it to its intensity in the cytosol. The intensity in the endosomes was set as 100%. Compared to the endosomes, the intensity of the C2 toxin in the cytosol of the treated cells was $21.4 \pm 8.4\%$ after 6 h. MTX ($6.3 \pm 2.5\%$) blocked this increase in intensity of C2 toxin staining after 6 h (mean \pm SEM; $n = 10$).

DISCUSSION

It is reported for several bacterial toxins, which act by modifying cytosolic substrates, that the B-subunit forms pores in lipid membranes. However, the role of these pores in the translocation of the A-subunit of the toxins across cell membranes is still enigmatic.

We use the binary *C. botulinum* C2 toxin to study the role of pores, which are formed by the binding/translocation component C2II for cellular uptake of the enzyme component C2I. C2II forms pores in artificial lipid bilayer membranes (24, 25) as well as in membranes of intact cells (26). These pores are cation-selective channels (25), which are inserted into membranes in an oriented manner; i.e., they have a cis and a trans site (27). Pore formation was restricted to the proteolytic activated heptameric form C2IIa (17). Moreover, pore formation of C2IIa in cell membranes depended on binding of C2IIa to its cellular receptor and on an acidic impulse to allow membrane insertion of C2IIa (26).

We studied the role of C2IIa pores for translocation of the enzyme component C2I and found that pore formation was an essential prerequisite for uptake of C2I into the cytosol (26). C2I normally translocates from acidic endosomal compartments into the cytosol of target cells, a step which can be blocked by the fungal drug bafilomycin A1 (17), an inhibitor of the vesicular H^+ -ATPase. Most likely, C2IIa forms pores in endosomal membranes, which facilitate translocation of C2I. We used experimental conditions that mimic the acidic endosomes to study the mechanism of C2IIa-mediated translocation of C2I in more detail. In these experiments, we used a short extracellular pulse to deliver C2I (via C2IIa) directly across cell membranes into the cytosol and observed cell rounding by ADP-ribosylation of actin (17).

In the present paper we report that unfolding of a C2I-DHFR fusion toxin is an essential prerequisite for its cytotoxic action in the cytosol. In this protein, DHFR represents a folded domain whose stability can be manipulated by addition of the ligand MTX. Without MTX, the C2I-DHFR fusion toxin (71 kDa) showed cytotoxic activity

similar to that of wild-type C2I when it was applied to cells together with C2IIa. This indicates that the DHFR domain did not diminish C2IIa-mediated translocation of the toxin into the cytosol. Binding of the folate analogue MTX to DHFR stabilizes the conformation of the DHFR domain, prevents its unfolding, and makes the protein resistant for proteolytic cleavage. When Vero cells were treated with C2IIa together with C2I-DHFR in the presence of MTX, intoxication was significantly delayed. MTX did not reduce cell binding of radiolabeled C2I-DHFR. Moreover, MTX did not decrease ADP-ribosylation of actin from Vero cell lysates by the C2I-DHFR fusion toxin *in vitro*. The presence of MTX diminished the direct translocation of C2I-DHFR across cell membranes through C2IIa. This direct translocation is driven by an acidic pulse and mimics the endosomal conditions. Most likely, binding of MTX to the DHFR domain keeps the fusion toxin in the folded conformation and thereby blocks translocation across endosomal membranes (see the model in Figure 6A). However, the inhibitory effect of MTX on toxin translocation was transient. One reason for this might be the special properties of bacterial protein toxins. These toxins are extremely potent. After a certain time, very few toxin molecules may "escape" from the MTX binding and reach the cytosol of cells what leads to a complete intoxication of these cells. Various inhibitors (as geldanamycin or radicicol, which inhibit Hsp90) which we used in past studies on C2 toxin only had a transient effect and did not block intoxication of cells completely (19).

Recently, we reported that a stringent sequence of steps was absolutely essential for the delivery of C2I into the cytosol of target cells (26). C2I must be bound to C2IIa on the surface of cells prior to the acidic pulse, which induces translocation of C2I into the cytosol. Translocation of C2I was only detected when pores were formed by C2IIa (26). Moreover, C2I interacts with C2IIa pores *in vitro* and *in vivo*, and in the presence of C2I, the C2IIa channels are partially blocked (26). When the C2IIa pores were blocked by the inhibitor chloroquin, a reduced intoxication of cells was observed, suggesting that less C2I reached the cytosol (27). Taken together, these findings strongly suggest an important role of C2IIa pores for translocation of C2I, but it is still unclear whether C2I (49 kDa) translocates directly through the pores [inner diameter $\sim 1-2$ nm (17)]. If so, an unfolding of C2I during the translocation step should be expected (see Figure 6A). This notion is supported by our recent finding that the host cell chaperone Hsp90 is essential for delivery of C2I from acidic endosomes into the cytosol. Treatment of cells with the specific pharmacological inhibitors of Hsp90, geldanamycin or radicicol, protected cells from cytotoxic effects, and C2I was trapped in the endosomes (19). We believe that Hsp90 is involved in translocation and refolding of C2I to recover its ADP-ribosyltransferase activity in the cytosol. In summary, unfolding of C2I is essential for its translocation from acidic endosomes into the cytosol of target cells, and studies are underway to test whether the C2I protein translocates directly through the lumen of the pores formed by C2IIa.

Several bacterial toxins translocate their enzymatic moiety across cellular membranes by using pores, which are formed by the binding/translocation domain of these toxins. For the group of binary toxins such as the family of actin-ADP-ribosylating toxins and the anthrax toxins, pore

formation by the individual binding components in the membranes of acidic endosomes was reported. In the anthrax system, a central binding/translocation component, the protective antigen, PA, mediates delivery of two different enzyme components into the cytosol of target cells, the edema factor, EF, and the lethal factor, LF, respectively. EF is a calmodulin-dependent adenylyl cyclase (28), and LF is a metalloprotease (29), which cleaves MAP kinase kinase. PA shares significant sequence homology with C2II (3). Like C2IIa, following proteolytic activation, PA forms ring-shaped heptamers (30), which insert as pores in membranes under acidic conditions (31, 32). Moreover, like C2 toxin, the enzyme components of anthrax toxins translocate from early acidic endosomes into the cytosol. Membrane translocation of LF was characterized by Wesche and colleagues by the use of an LF_N-DHFR fusion protein (33). DHFR was fused to the N-terminal domain of LF, and translocation of this protein via PA was reduced by MTX (33). Therefore, despite the fact that C2I and LF represent completely different enzymes, they both translocate in a partially unfolded conformation across membranes, most likely through the pores formed by C2IIa and PA, respectively. Interestingly, we could not show an involvement of Hsp90 in the translocation of active LF into the cytosol (19), which is a remarkable difference to C2 toxin, whose translocation depends on Hsp90.

Pore formation by the binding/translocation domain of toxins and translocation of the enzymatically active moiety in an unfolded conformation is not restricted to binary toxins. In diphtheria toxin (DT), an α -helical transmembrane (T) domain forms pores in membranes under acidic conditions (34, 35). Recently, Ratts and colleagues reported that active Hsp90 is essential for translocation of the active domain of DT from acidic endosomes (36). However, it was never shown directly for any toxin that its enzymatic domain translocates directly through the pore. This remains one of the central questions for future studies on the translocation mechanism of bacterial protein toxins.

ACKNOWLEDGMENT

We thank Brigitte Neufang for expert technical assistance.

REFERENCES

- Montecucco, C., Papini, E., and Schiavo, G. (1994) *FEBS Lett.* 346, 92–98.
- Olsnes, S., Wesche, J., and Falnes, P. O. (2000) in *Bacterial Protein Toxins* (Aktories, K., and Just, I., Eds.) pp 1–19, Springer, Berlin.
- Barth, H., Blöcker, D., and Aktories, K. (2002) *Naunyn-Schmiedeberg's Arch. Pharmacol.* 366, 501–512.
- Ohishi, I., Miyake, M., Ogura, H., and Nakamura, S. (1984) *FEMS Microbiol. Lett.* 23, 281–284.
- Ohishi, I., Iwasaki, M., and Sakaguchi, G. (1980) *Infect. Immun.* 30, 668–673.
- Perelle, S., Gibert, M., Boquet, P., and Popoff, M. R. (1995) *Infect. Immun.* 63, 4967.
- Stiles, B. G., and Wilkens, T. D. (1986) *Infect. Immun.* 54, 683–688.
- Popoff, M. R., and Boquet, P. (1988) *Biochem. Biophys. Res. Commun.* 152, 1361–1368.
- Stiles, B. G., and Wilkins, T. D. (1986) *Toxicon* 24, 767–773.
- Gülke, I., Pfeifer, G., Liese, J., Fritz, M., Hofmann, F., Aktories, K., and Barth, H. (2001) *Infect. Immun.* 69, 6004–6011.
- Popoff, M. R., Rubin, E. J., Gill, D. M., and Boquet, P. (1988) *Infect. Immun.* 56, 2299–2306.
- Han, S., Craig, J. A., Putnam, C. D., Carozzi, N. B., and Tainer, J. A. (1999) *Nat. Struct. Biol.* 6, 932–936.
- Aktories, K., Bärmann, M., Ohishi, I., Tsuyama, S., Jakobs, K. H., and Habermann, E. (1986) *Nature* 322, 390–392.
- Wegner, A., Aktories, K., Ditsch, A., Just, I., Schoepper, B., Selve, N., and Wille, M. (1994) *Adv. Exp. Med. Biol.* 358, 97–104.
- Ohishi, I. (2000) in *Bacterial Protein Toxins* (Aktories, K., and Just, I., Eds.) pp 253–273, Springer-Verlag, Berlin.
- Ohishi, I. (1987) *Infect. Immun.* 55, 1461–1465.
- Barth, H., Blöcker, D., Behlke, J., Bergsma-Schutter, W., Brisson, A., Benz, R., and Aktories, K. (2000) *J. Biol. Chem.* 275, 18704–18711.
- Eckhardt, M., Barth, H., Blöcker, D., and Aktories, K. (2000) *J. Biol. Chem.* 275, 2328–2334.
- Haug, G., Leemhuis, J., Tiemann, D., Meyer, D. K., Aktories, K., and Barth, H. (2003) *J. Biol. Chem.* 274, 32266–32274.
- Eilers, M., and Schatz, G. (1986) *Nature* 322, 228–232.
- Matouschek, A., Pfanner, N., and Voos, W. (2000) *EMBO Rep.* 1, 404–410.
- Barth, H., Preiss, J. C., Hofmann, F., and Aktories, K. (1998) *J. Biol. Chem.* 273, 29506–29511.
- Hildebrand, B., Olenik, C., Uhl, A., and Meyer, D. K. (1997) *Brain Res.* 759, 285–291.
- Blöcker, D., Behlke, J., Aktories, K., and Barth, H. (2001) *Infect. Immun.* 69, 2980–2987.
- Schmid, A., Benz, R., Just, I., and Aktories, K. (1994) *J. Biol. Chem.* 269, 16706–16711.
- Blöcker, D., Pohlmann, K., Haug, G., Bachmeyer, C., Benz, R., Aktories, K., and Barth, H. (2003) *J. Biol. Chem.* 278, 37360–37367.
- Bachmeyer, C., Benz, R., Barth, H., Aktories, K., Gibert, M., and Popoff, M. (2001) *FASEB J.* 15, 1658–1660.
- Leppla, S. (1982) *Proc. Natl. Acad. Sci. U.S.A.* 79, 3162–3166.
- Duesbery, N. S., Webb, C. P., Leppla, S. H., Gordon, V. M., Klimpel, K. R., Copeland, T. D., Ahn, N. G., Oskarsson, M. K., Fukasawa, K., Paull, K. D., and Woude, G. F. V. (1998) *Science* 280, 734–737.
- Petosa, C., Collier, R. J., Klimpel, K. R., Leppla, S. H., and Liddington, R. C. (1997) *Nature* 385, 833–838.
- Milne, J. C., and Collier, R. J. (1993) *Mol. Microbiol.* 10, 647–653.
- Miller, C. J., Elliott, J. L., and Collier, R. J. (1999) *Biochemistry* 38, 10432–10441.
- Wesche, J., Elliott, J. L., Falnes, P. O., Olsnes, S., and Collier, R. J. (1998) *Biochemistry* 37, 15737–15746.
- Kagan, B. L., Finkelstein, A., and Colombini, M. (1981) *Proc. Natl. Acad. Sci. U.S.A.* 78, 4950–4954.
- Oh, K. J., Senzel, L., Collier, R. J., and Finkelstein, A. (1999) *Proc. Natl. Acad. Sci. U.S.A.* 96, 8467–8470.
- Ratts, R., Zeng, H., Berg, E. A., Blue, C., McComb, M. E., Costello, C. E., Vanderspek, J. C., and Murphy, J. R. (2003) *J. Cell Biol.* 160, 1139–1150.

BI0354278